Research Article

BIOMEDICAL Journal of Scientific & Technical Research

ISSN: 2574 -1241

DOI: 10.26717/BJSTR.2023.51.008046

Impact of Contaminated Surfaces on the Transmission Dynamics of Corona Virus Disease (Covid-19)

Idowu, Kabir Oluwatobi[1]*, Loyinmi, Adedapo Chris[2]

[1]*Department of Mathematics, Purdue University, USA*

[2]*Department of Mathematics, Tai Solarin University of Education, Ijagun, Ogun state. Nigeria.*

***Corresponding author:** Idowu Kabir Oluwatobi, Department of Mathematics, Purdue University, USA

ARTICLE INFO

Received: June 07, 2023

Published: June 15, 2023

Citation: Idowu Kabir Oluwatobi and Loyinmi, Adedapo Chris. Impact of Contaminated Surfaces on the Transmission Dynamics of Corona Virus Disease (Covid-19). Biomed J Sci & Tech Res 51(1)-2023. BJSTR. MS.ID.008046.

ABSTRACT

We assumed a homogeneously mixed population and that the disease does not only spread by direct contact with an infected individual but also by touching infected surfaces (environment). We then propose an SQEIRVS model and validate correlation between upsurge in transmission and touching surfaces contaminated by droplets from COVID-19 infected individual. We performed the appropriate analyses for positivity and boundedness, reproduction number, and stability. The problem was modelled numerically. Furthermore, we identified the criteria required for the stability of both DFE and endemic equilibrium. Asymptotically, the DFE is stable. Additionally, the endemic equilibrium is stable. The numerical results showed that treatment and immunization are effective in reducing the spread of the infections.

Keywords: Covid 19 Transmission; Disease Free Equilibrium; Endemic Equilibrium; Stability Analysis; Environmental Factor

Abbreviations: CoVs: Coronaviruses; SARS-CoV2: Severe Acute Respiratory Syndrome Coronavirus-2; SARS: Severe Acute Respiratory Syndrome; MERS-CoV: Middle East Respiratory Syndrome-Cov; WHO: World Health Organization; E: Exposed; I: Infectious; CDC: Centers for Control and Prevention

Introduction

According to Anthony RF [1], coronaviruses are regarded as the largest group of viruses belonging to the Nidovirales order, which includes the Coronaviridae, Arteriviridae, Mesoniviridae, and Roniviridae families. Coronavirus virions are circular, with a diameter of nearly 125 nm. The most conspicuous characteristic of coronaviruses is the club-shaped spiked projections originating from the surface of the virion. Such spikes are regarded as one of the definite characteristics of the virion, which gives them the appearance of a solar corona, thus leading to the term coronaviruses. The virion, called Coronaviridae, is found in a broad range of hosts and carriers, infecting many avian species and subspecies and even mammals. This virus most often affects the upper respiratory, gastrointestinal, hepatic, and central nervous systems through a number of diseases (Gallagher [2-5]). Hassan [3] stated that the human types of coronavirus are linked to minor clinical symptoms (Akinfe [6-12]). At the same time, the Coronaviridae family is divided into two, which include Torovirinae and Coronavirinae (Akinfe [13-15]). Further, the Coronavirinae subfamily is classified into alpha-, beta-, gamma-, and delta-COVs (Lawal, et al. [16-19]. These viruses have a virus-related RNA genome that measures from 26 to 32 kilobases in dimension, and this makes it possible to isolate them from different animal species. Moreover, the coronaviruses can be seen under the electron microscope as they possess a crown-like appearance. Ideally, the extensive spread and associated health risks of the disease make it an essential pathogen. The coronavirus disease 2019 (COVID-19) is a pandemic and has its origins in Wuhan Province, China, in late 2019.

It is, however, caused by the severe acute respiratory syndrome coronavirus-2 (SARS-CoV2). As of June 6, 2020, the number of confirmed cases worldwide was 66,63,204, with over 392802 deaths, as per the WHO COVID-19 Dashboard (Lawal [20, 21]). The U.S.A. has the largest number of cases worldwide, with over 18,57,772 cases

and 107911 deaths, followed by Brazil and Russia with 6,14,941 and 4,58,869 confirmed cases, respectively (Lawal, et al. [22, 23]). China, where the pandemic began, has reported 84,620 confirmed cases and 4,645 deaths to date. In India, there have been 2,36,657 total cases with over 6,642 deaths till now (6 June 2020). This pandemic has led to worldwide lockdown, strangling of the global economy, and devastation of human life (Atri [24]). Going down the history lane, SARS-CoV, a group 2b coronavirus, was detected as the potential cause of the 2002–2003 outbreak of Severe Acute Respiratory Syndrome (SARS) in the Guangdong Province of China. In a cluster of highly pathogenic respiratory tract infections in Saudi Arabia and other countries in the Middle East throughout 2012, Middle East Respiratory Syndrome-CoV (MERS-CoV) was found to be the potential cause and is an example of another novel human CoV (Zaki AM [26]). Rismanbaf A. [27] stated that the World Health Organisation (WHO) officially named the disease the coronavirus disease 2019 (COVID-19) on February 11, 2020. World Health Organization (WHO) also announced a global emergency on January 31st due to increasing concern about its rapid spread, and the disease became listed as a pandemic on March 11th, 2020.

As per WHO, the Centres for Disease Control and Prevention (CDC), and the FDA, there are presently no drugs or vaccinations that are known to be successful for SARS-CoV-2 management or preventing the spread. Within clinical trials and compassionate use guidelines, numerous different compounds are used based on their in vitro activity (against SARS-CoV-2 or associated viruses) and on constrained clinical knowledge (Loyinmi [28]). Gallagher TM [29] stated that the origin of the virus has been attributed to exposure to the Huanan seafood market, which was common among the earliest cases contributing to the SARSCoV2 epidemic in China. According to Rismanbaf A [30], mathematical modelling has become an important tool in understanding the dynamics of disease transmission and in decision making processes regarding intervention programmes for disease control. Mathematical models provide a framework for understanding the transmission dynamics of diseases.

Model Formulation

In this study, we considered an SQEIRVS Model with restriction in the recruitment rate into the population [9]. We assumed that the population is homogeneously mixed and that the disease does not only spread through direct contact with an infected individual but also through contact with an infected surface (environment) [10]. Droplets from sneezing infected individual contaminate surfaces and which is the reason behind world-wide mask wearing to prevent direct infection and also contaminating nearby surfaces when sneezing or talking in public [11]. In this study, P(t) denotes the total number of human population at time (t), S(t) denotes susceptible individuals, Q(t) is the Quarantined humans, E(t) is the Exposed humans' population, I(t) is the Infectious human population, R(t) represents Recovered humans and V(t) denotes virus's infections in the environment [12].

ϕ is the rate of contact of human with the environment. ε_1 is the rate of human contact with infectious area of the environment while ε_2 is the rate of contact exposed and infectious human with the environment [13]. β_1 denotes the probability of human getting infected when in contact with environment while β_2 is the probability of the environment getting infected when in contact with human [14]. μ is per capita natural death rate of human, δ is per capita rate of loss of immunity by recovered individuals. λ_h denotes the force of infection for susceptible human when in contact with an infected human while λ_e represents the force of infection for susceptible human when in contact with an infected environment [15].

λ is the force of infection i.e. $\lambda = \lambda_h + \lambda_e$ (1)

Where $\lambda_h = \beta_1 \varepsilon_1 \phi I(t)$ and $\lambda_e = \beta_2 \varepsilon_2 \phi V(t)$ (2)

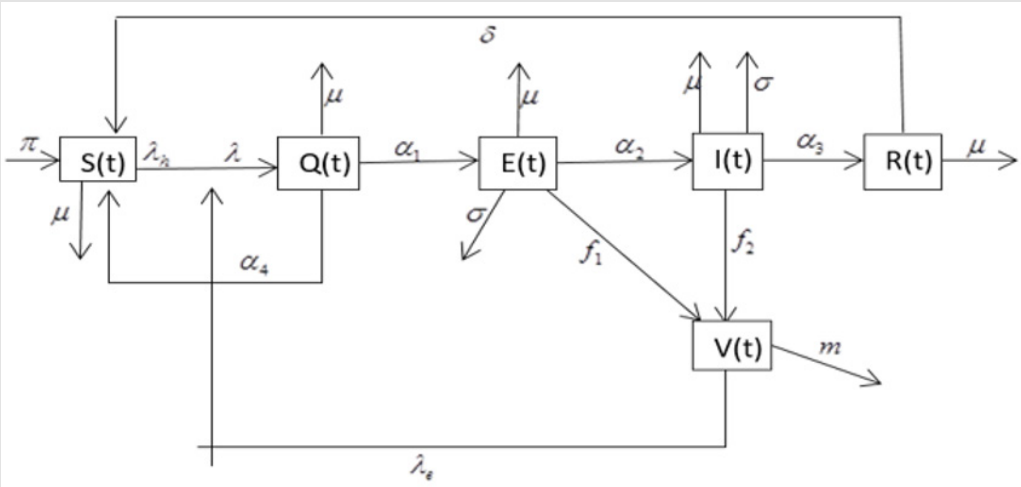

Figure 1: Compartmental diagram for the transmission dynamics of COVID 19.

progress to the exposed compartment at the rate of α_1 while those who tested negative move back to the susceptible class at the rate α_4 . Exposed individuals progress to the infectious class at the rate of α_2 . Infectious human are recovered at the rate while COVID 19 induce death rate is assumed to be σ [17]. Also, $f_i, i = 1,2$ is the rate of virus in the environment from both the exposed (E) and infectious (I) class and the virus is removed from the environment at the rate m [18] (Figure 1).

Therefore, the dynamics of the model is presented below as a system of non-linear differential equation

$$\frac{dS(t)}{dt} = \pi - \lambda(H)S(t) - \mu S(t) + \alpha_4 Q(t) + \delta R(t)$$

$$\frac{dQ(t)}{dt} = \lambda(H)S(t) - (\alpha_4 + \mu + \alpha_1)Q(t)$$

$$\frac{dE(t)}{dt} = \alpha_1 Q(t) - (\alpha_2 + \sigma + \mu)E(t)$$

$$\frac{dI(t)}{dt} = \alpha_2 E(t) - (\sigma + \mu + \alpha_3)I(t)$$

$$\frac{dR(t)}{dt} = \alpha_3 I(t) - (\delta + \mu)R(t)$$

$$\frac{dV(t)}{dt} = f_1 E(t) + f_2 I(t) - mV(t) \quad (3)$$

Model Analysis

Under this section, we consider the positivity and boundedness of the solution of model, we also consider the reproduction number and the stability of the disease free equilibrium and endemic equilibrium [19].

Positivity and Boundedness of Solution

We hereby present a lemma for the positivity and boundedness of the solution of the model as follows:

Lemma 1: The solution S(t), Q(t), E(t), I(t), R(t), and V(t) of system [1] with the initial condition S(0) > 0, Q(0) > 0, E(0) > 0, I(0) > 0, R(0) > 0 and V(0) > 0 are all positive for all t > 0.

Proof : From system [1] First equation

$\frac{dS(t)}{dt} = \pi - \lambda(H)S(t) - \mu S(t) + \alpha_4 Q(t) + \delta R(t)$ That is

$$\frac{dS(t)}{dt} = (\lambda(H) + \mu)S(t) \geq 0$$

$\frac{d}{dt}\left[Se^{(\lambda(H)+\mu)t}\right] \geq 0, \quad Se^{(\lambda(H)+\mu)t} \geq c, \quad S(t) \geq ce^{-(\lambda(H)+\mu)t}$ At t=o $S(t) \geq S(0)e^{-(\lambda(H)+\mu)t} \geq 0$

Therefore $S(t) \geq 0$ (Thus $S(t)$ stays positive).

Let $(\alpha_4 + \mu + \alpha_1) = \Omega, \ \frac{dQ(t)}{dt} = \lambda(H)S(t) - \Omega Q(t)$ That is $\frac{dQ(t)}{dt} \geq -\Omega Q(t)$

$\frac{d}{dt}\left[Q(t)e^{\Omega t}\right] \geq 0$ At t=0, $Q(t) \geq Q(0)e^{-\Omega t} \geq 0$ Therefore $Q(t) \geq 0$ (Thus $Q(t)$ stays positive).

Let $(\alpha_2 + \sigma + \mu) = \varphi$, $\frac{dE(t)}{dt} = \alpha_1 Q(t) - \varphi E(t)$,That is $\frac{dE(t)}{dt} \geq -\varphi E(t)$,Then $\frac{dE(t)}{dt} + \varphi E(t) \geq 0$

$\frac{d}{dt}\left[E(t)e^{\varphi t}\right] \geq 0$, At t=0, $E(t) \geq E(0)e^{-\varphi t} \geq 0$, Therefore $E(t) \geq 0$ (Thus $E(t)$ stays positive).

Let $(\alpha_3 + \sigma + \mu) = \omega$, $\frac{dI(t)}{dt} = \alpha_2 E(t) - \omega I(t)$, That is $\frac{dI(t)}{dt} \geq -\omega I(t)$, Then $\frac{dI(t)}{dt} + \omega I(t) \geq 0$,

$\frac{d}{dt}\left[I(t)e^{\omega t}\right] \geq 0$, At t=0, $I(t) \geq I(0)e^{-\omega t} \geq 0$ Therefore $I(t) \geq 0$ (Thus $I(t)$ stays positive).

$\frac{dR(t)}{dt} = \alpha_3 I(t) - (\delta + \mu)R(t)$, That is $\frac{dR(t)}{dt} \geq -(\delta + \mu)R(t)$, Then $\frac{dR(t)}{dt} + (\delta + \mu)R(t) \geq 0$,

$\frac{d}{dt}\left[R(t)e^{(\delta+\mu)t}\right]\geq 0$ Integrating both sides, we have $R(t)e^{(\delta+\mu)t}\geq c$, $R(t)\geq e^{-(\delta+\mu)t}$

At t=0, $R(t)\geq R(0)e^{-(\delta+\mu)t}\geq 0$ Therefore $R(t)\geq 0$ (Thus $R(t)$ stays positive).

$\frac{dV(t)}{dt}=f_1E(t)+f_2I(t)-mV(t)$ That is $\frac{dV(t)}{dt}\geq -mV(t)$, $V(t)\geq V(0)e^{-mt}\geq 0$ Therefore

$V(t)\geq 0$ (Thus $V(t)$ stays positive).

Now, $P(t)=S(t)+Q(t)+E(t)+I(t)+R(t)$, Thus $P(t)\geq 0$

This is sufficient to show that P(t) is bounded in the region R^+ and it remains positive for all values of $t\geq 0$

$$P(t)=S(t)+Q(t)+E(t)+I(t)+R(t)$$

$$\frac{P(t)}{dt}=\pi-\mu\left(S(t)+Q(t)+E(t)+I(t)+R(t)\right)$$
$$-\sigma\left(E(t)+I(t)\right),$$

$$\frac{P(t)}{dt}=\pi-\mu P(t)-\sigma\left(E(t)+I(t)\right)$$

$$\frac{P(t)}{dt}+\mu P(t)\leq\pi,\ \frac{d}{dt}\left[P(t)e^{\mu t}\right]\leq\pi e^{\mu t}$$

Integrating both sides gives $P(t)e^{\mu t}\leq\frac{\pi}{\mu}e^{\mu t}+C$

Therefore, $P(t)\leq\frac{\pi}{\mu}\left(1+Ce^{-\mu t}\right)$ where C is the constant of integration $\lim_{t\to\infty}p(t)\leq\frac{\pi}{\mu}\left(1+Ce^{-\infty t}\right)=\lim_{t\to\infty}p(t)\leq\frac{\pi}{\mu}(1)=\frac{\pi}{\mu}$ (4)

This proves the boundedness of the solution inside R [20]. This implies solutions of the system are positive. Thus R is positive invariant and attracting and hence, it is sufficient to consider the dynamics of the system [21].

Disease Free Equilibrium Points (DFE)

To obtain the Disease free equilibrium, we set all class to zero apart from the susceptible class [22].

$$\pi-\mu S^0=0 \quad (5)$$

That is $S^0=\frac{\pi}{\mu}$

The DFE point of the system is

$$E_0=\left(S^0+Q^0+E^0+I^0+R^0+V^0\right)=\left(\frac{\pi}{\mu},0,0,0,0,0,\right) \quad (6)$$

Now let us check if the DFE point actually exists for system [1]

Existence of Equilibrium (Critical) Point

We obtain the equilibrium points of system [1] by solving, equating the rate of change with respect to time (t) of all dynamical variables to zero [23].

$$\pi-\lambda(H)S(t)-\mu S(t)+\alpha_4Q(t)+\delta R(t)=0 \quad (7)$$

$$\lambda(H)S(t)-\Omega Q(t)=0 \quad (8)$$

$$\alpha_1Q(t)-\phi E(t)=0 \quad (9)$$

$$\alpha_2E(t)-\omega I(t)=0 \quad (10)$$

$$\alpha_3I(t)-(\delta+\mu)R(t)=0 \quad (11)$$

$$f_1E(t)+f_2I(t)-mV(t)=0 \quad (12)$$

Therefore $R(t)=\frac{\pi\lambda(H)\alpha_1\alpha_2\alpha_3}{A_1\lambda+A_0}$ (13)

$$I(t)=\frac{(\delta+\mu)\pi\lambda(H)\alpha_1\alpha_2}{\left(A_1\lambda+A_0\right)} \quad (14)$$

$$E(t)=\frac{\omega(\delta+\mu)\pi\lambda(H)\alpha_1}{\left(A_1\lambda+A_0\right)} \quad (15)$$

$$Q(t)=\frac{\phi\omega(\delta+\mu)\pi\lambda(H)}{\left(A_1\lambda+A_0\right)} \quad (16)$$

$$S(t)=\frac{\Omega\phi\omega(\delta+\mu)\pi}{A_1\lambda+A_0} \quad (17)$$

$$V(t)=\frac{(\delta+\mu)\pi\lambda(H)\alpha_1\left(f_1\omega+f_2\alpha_2\right)}{m\left(A_1\lambda+A_0\right)} \quad (18)$$

where

$A_0=\varphi\omega(\delta+\mu)\Omega\mu$, $A_1=((\varphi\omega(\delta+\mu)(\Omega-\alpha_4))-\lambda\alpha_1\alpha_2\alpha_3)$, $A_2=(\delta+\mu)\pi\alpha_1(f_1\omega+f_2\alpha_2)$ and $A_3=(\delta+\mu)\pi\alpha_{12}\alpha_2$

Recall that $\lambda(H)=\lambda_h+\lambda_e$ and $\lambda=\varphi\left(\varepsilon_1\beta_1V(t)+\varepsilon_2\beta_2I(t)\right)$

$$\lambda(H)=\varphi\begin{pmatrix}\varepsilon_1\beta_1\dfrac{(\delta+\mu)\pi\lambda(H)\alpha_1\left(f_1\omega+f_2\alpha_2\right)}{m\left(A_1\lambda+A_0\right)}\\+\varepsilon_2\beta_2\dfrac{(\delta+\mu)\pi\lambda(H)\alpha_1\alpha_2}{\left(A_1\lambda+A_0\right)}\end{pmatrix} \quad (19)$$

$$\lambda(H)=\varphi\lambda(H)\left(\frac{\varepsilon_1\beta_1A_2+m\varepsilon_2\beta_2A_3}{m\left(A_1\lambda+A_0\right)}\right)$$

$$\Rightarrow mA_1\lambda^2(H)+mA_0\lambda(H)=\varphi\left(\varepsilon_1\beta_1A_2+m\varepsilon_2\beta_2A_3\right)\lambda(H)$$

$$mA_1\lambda^2(H)+\left(mA_0-\varphi\left(\varepsilon_1\beta_1A_2+m\varepsilon_2\beta_2A_3\right)\right)\lambda(H)=0$$

$$\lambda^2(H)+\frac{\left(mA_0-\varphi\left(\varepsilon_1\beta_1A_2+m\varepsilon_2\beta_2A_3\right)\right)}{mA_1}\lambda(H)=0$$

$$\lambda(H)\left(\lambda(H)+\frac{\left(mA_0-\varphi\left(\varepsilon_1\beta_1A_2+m\varepsilon_2\beta_2A_3\right)\right)}{mA_1}\right)=0$$

$$\lambda(H)=0 \text{ or } \lambda(H)=\frac{\varphi\left(\varepsilon_1\beta_1A_2+m\varepsilon_2\beta_2A_3\right)-mA_0}{mA_1} \quad (20)$$

Case 1 $\lambda(H)=0$

Then from (6) to (11), we observed that $E_0=\left(\frac{\pi}{\mu},0,0,0,0,0,\right)$

Therefore, the disease free equilibrium point [24], exist and this represent a state where there is no presence of the novel corona virus disease in the population i.e. the infectious class equals zero [25].

Reproduction Number R_0

Using the next generation matrix method [26], we determine the basic reproduction number R_0 and the control reproduction number R_c of the model [27]. The matrices P and V denoting the new infection term and the remaining transfer terms at the disease free equilibrium respectively are given by

$$P=\begin{bmatrix}\lambda S\\0\\0\\f_1E+f_2I\end{bmatrix}\quad V=\begin{bmatrix}(\alpha_4+\mu+\alpha_1)Q\\(\alpha_2+\sigma+\mu)E-\alpha_1Q\\-\alpha_2E+(\sigma+\mu+\alpha_3)I\\mV\end{bmatrix} \quad (21)$$

Consequently, we have the next generation matrix

$$P=\begin{bmatrix}0&0&\dfrac{\beta_1\varepsilon_1\varphi\pi}{\mu}&\dfrac{\beta_2\varepsilon_2\varphi\pi}{\mu}\\0&0&0&0\\0&0&0&0\\0&f_1&f_2&0\end{bmatrix} \text{ and}$$

$$V=\begin{bmatrix}w_1&0&0&0\\-\alpha_1&w_2&0&0\\0&-\alpha_2&w_3&0\\0&0&0&m\end{bmatrix} \quad (22)$$

Where

$w_1=\alpha_4+\mu+\alpha_1$, $w_2=\alpha_2+\sigma+\mu+f_1$, $w_3=\sigma+\mu+f_2+\alpha_3$, $w_4=\delta+\mu$ (23)

$$V^{-1}=\begin{bmatrix}\dfrac{1}{w_1}&0&0&0\\\dfrac{\alpha_1}{w_1w_2}&\dfrac{1}{w_2}&\dfrac{\alpha_2}{w_2w_3}&0\\\dfrac{\alpha_1\alpha_2}{w_1w_2w_3}&0&\dfrac{1}{w_3}&0\\0&0&0&\dfrac{1}{m}\end{bmatrix} \quad (24)$$

$$PV^{-1}=\begin{bmatrix}\dfrac{\beta_1\varepsilon_1\varphi\pi\alpha_1\alpha_2}{\mu w_1w_2w_3}&0&\dfrac{\beta_1\varepsilon_1\varphi\pi}{\mu w_3}&\dfrac{\beta_2\varepsilon_2\varphi\pi}{\mu m}\\0&0&0&0\\0&0&0&0\\\dfrac{f_1\alpha_1}{w_1w_2}+\dfrac{f_2\alpha_1\alpha_2}{w_1w_2w_3}&\dfrac{f_1}{w_2}&\dfrac{f_1\alpha_2}{w_2w_3}+\dfrac{f_2}{w_3}&0\end{bmatrix} \quad (25)$$

$$R_0 = \rho(PV^{-1}) = \frac{\alpha_1\beta_2\varepsilon_2\varphi\pi\left(f_1w_3 + f_2\alpha_2\right) + m\alpha_2\alpha_1\beta_1\varepsilon_1\varphi\pi}{\mu m w_3 w_2 w_1} \quad (26)$$

Stability of Disease Free Equilibrium (DFE)

Theorem 1: The DFE point of the system is locally asymptomatically stable whenever $R_0 < 1$

Proof: Let

$$\begin{aligned} F_1 &= \pi - \lambda(H)S(t) - \mu S(t) + \alpha_4 Q(t) + \delta R(t) \\ F_2 &= \lambda(H)S(t) - (\alpha_4 + \mu + \alpha_1)Q(t) \\ F_3 &= \alpha_1 Q(t) - (\alpha_2 + \sigma + \mu + f_1)E(t) \\ F_4 &= \alpha_2 E(t) - (\sigma + \mu + f_2 + \alpha_3)I(t) \\ F_5 &= \alpha_3 I(t) - (\delta + \mu)R(t) \\ F_6 &= f_1 E(t) + f_2 I(t) - mV(t) \end{aligned} \quad (27)$$

We use the Jacobian of the model evaluated at DFE to establish the local stability of the DFE [28]. The stability is determined based on the eigenvalue of the corresponding Jacobian which are functions of the model parameters [29].

$$J_0(F) = \begin{bmatrix} -\mu & \alpha_4 & 0 & -\gamma & \delta & -\eta \\ 0 & -w_1 & 0 & \gamma & 0 & \eta \\ 0 & \alpha_1 & -w_2 & 0 & 0 & 0 \\ 0 & 0 & \alpha_2 & -w_3 & 0 & 0 \\ 0 & 0 & 0 & \alpha_3 & -w_4 & 0 \\ 0 & 0 & f_1 & f_2 & 0 & -m \end{bmatrix}$$

Where, $\frac{\beta_1\varepsilon_1\phi\pi}{\mu} = \gamma, \frac{\beta_2\varepsilon_2\phi\pi}{\mu} = \eta$ (28)

Clearly, we see that the eigenvalues are $\lambda_1 = -\mu, \lambda_2 = -w_4$ then we have the matrix [30].

$$M = \begin{bmatrix} -w_1 & 0 & \gamma & \eta \\ \alpha_1 & -w_2 & 0 & 0 \\ 0 & \alpha_2 & -w_3 & 0 \\ 0 & f_1 & f_2 & -m \end{bmatrix}$$

The characteristic equation of the matrix is

$$\lambda^4 + A_1\lambda^3 + A_2\lambda^2 + A_3\lambda + A_4 \quad (29)$$

$$A_1 = m + w_3 + w_2 + w_1,\ A_2 = mw_3 + mw_2 + mw_1 + w_3w_2 + w_3w_1 + w_2w_1$$

$$A_3 = -f_1\alpha_1\eta + mw_3w_2 + mw_3w_1 + mw_2w_1 - \alpha_2\alpha_1\gamma + w_3w_2w_1$$

$$A_4 = -f_2\alpha_1\alpha_2\eta - f_1\alpha_1\eta w_{31} - m\alpha_2\alpha_1\gamma + mw_3w_2w_1$$

$$A_4 = -f_2\alpha_1\alpha_2\frac{\beta_2\varepsilon_2\varphi\pi}{\mu} - f_1\alpha_1\frac{\beta_2\varepsilon_2\varphi\pi}{\mu}w_3 - m\alpha_2\alpha_1\frac{\beta_1\varepsilon_1\varphi\pi}{\mu} + mw_3w_2w_1$$

On simplification,

$$A_4 = -f_2\alpha_1\alpha_2\frac{\beta_2\varepsilon_2\phi\pi}{\mu} - f_1\alpha_1\frac{\beta_2\varepsilon_2\phi\pi}{\mu}w_3 - m\alpha_2\alpha_1\frac{\beta_1\varepsilon_1\phi\pi}{\mu} + mw_3w_2w_1$$

$$mw_3w_2w_1\left(1 - \frac{\alpha_1\beta_2\varepsilon_2\varphi\pi\left(f_1w_3 + f_2\alpha_2\right) + m\alpha_2\alpha_1\beta_1\varepsilon_1\varphi}{\mu m w_3 w_2 w_1}\right.$$

Therefore we have

$$mw_3w_2w_1\left(1 - R_0\right) > 0 \text{ if } R_0 < 1 \quad (30)$$

Where $R_0 = \frac{\alpha_1\beta_2\varepsilon_2\varphi\pi\left(f_1w_3 + f_2\alpha_2\right) + m\alpha_2\alpha_1\beta_1\varepsilon_1\varphi\pi}{\mu m w_3 w_2 w_1}$

Thus the eigenvalues of the model are real and negative if $R_0 < 1$ [31], therefore the DFE is locally asymptotically stable and unstable if $R_0 > 1$.

Stability of Disease Endemic Equilibrium (DEE)

Theorem 1: The DEE point of the system is locally asymptomatically stable whenever $R_0 > 1$

Proof: At the endemic equilibrium, we have the Jacobian matrix to be

$$J^*(F) = \begin{bmatrix} -\left(\lambda(H)^* + \mu\right) & \alpha_4 & 0 & -\beta_1\varepsilon_1\varphi S^* & \delta & -\beta_2\varepsilon_2\varphi S^* \\ \lambda(H)^* & -w_1 & 0 & \beta_1\varepsilon_1\varphi S^* & 0 & \beta_2\varepsilon_2\varphi S^* \\ 0 & \alpha_1 & -w_2 & 0 & 0 & 0 \\ 0 & 0 & \alpha_2 & -w_3 & 0 & 0 \\ 0 & 0 & 0 & \alpha_3 & -w_4 & 0 \\ 0 & 0 & f_1 & f_2 & 0 & -m \end{bmatrix} \quad (31)$$

The characteristic equation is given by $\left|J^{*}-I\lambda\right|=0$

From here [32], we shall use the property of R_0 to analyze the stability of the endemic equilibrium states ((Feng et al., (200`)). When $R_0>1$ [33], the system has a unique endemic equilibrium that is globally asymptotically stable [34]. So, from above,

$$R_0=\frac{\alpha_1\beta_2\varepsilon_2\varphi\pi\left(f_1w_3+f_2\alpha_2\right)+m\alpha_2\alpha_1\beta_1\varepsilon_1\varphi\pi}{\mu mw_3w_2w_1}$$

$$\frac{\alpha_1\beta_2\varepsilon_2\varphi\pi\left(f_1w_3+f_2\alpha_2\right)+m\alpha_2\alpha_1\beta_1\varepsilon_1\varphi\pi}{\mu mw_3w_2w_1}>1 \quad (32)$$

$$\alpha_1\beta_2\varepsilon_2\varphi\pi\left(f_1w_3+f_2\alpha_2\right)+m\alpha_2\alpha_1\beta_1\varepsilon_1\varphi\pi>\mu mw_3w_2w_1 \quad (33)$$

The inequality above gives the necessary and sufficient condition for the endemic equilibrium of the model to be globally asymptotically stable [35]. It is therefore interpreted as the product of the contraction and total breakdown of the susceptible class must be greater than the total removal rate for the quarantined class, Exposed class, Infectious class and the environment for the model to be globally asymptotically stable [36]. Therefore we must ensure that the endemic equilibrium state is never stable [37].

Numerical Simulation

The numerical simulation of the dynamics of this COVID-19 model over time was implemented with Maple software using the Runge-kutta-felhberg of fourth-fifth order (RKR-45) with degree four interpolant [38]. We make use of the variables in (Table 1) and the parameters given in (Table 2) in simulation based on the data provided [39]. Some values assigned to the parameter were derived from epidemiological literatures while others were estimated [40].

Table 1: Description of variables in the system in system [3].

State variables	Description
$S(t)$	Susceptible Human
$Q(t)$	Quarantined Human
$E(t)$	Exposed Humans
$I(t)$	Infectious Human
$R(t)$	Recovered Humans
$V(t)$	Virus in the Environment

Table 2: Symbols and Values of parameters used in the model.

Description of Parameter	Symbols	Value	Source
Recruitment rate	π	0.02461	Estimated
Natural death rate of humans	μ	0.0122	Adeniyi (2020)
Rate in which immunity is lost	δ	0.4335	Adeniyi (2020)
Rate of COVID-19 induced death	σ	0.1139	Adeniyi (2020)
Rate of progressive quarantined individuals to the exposed class	α_1	0.5	Estimated
Rate of progressive exposed individuals to the infectious class	α_2	0.56	Adeniyi (2020)
Recovery rate of infectious individuals	α_3	0.547	Estimated
Rate of progressive quarantined individuals to the susceptible class	α_4	0.56	Assumed
Rate of virus in the environment from the exposed	f_1	0.845	Estimated
Rate of virus in the environment from the infectious class	f_2	0.799	Estimated
Rate of removal of virus from the environment	m	0.975	Assumed

Discussion of Findings

As seen in (Figure 2), when the viral load in the environment rises, the vulnerable population decreases. However, after a certain amount of time (60 days), the quarantine, exposed, infected, and recovered categories do not change. This demonstrates that the virus is a serious danger to the infected person since the infectious population is decreasing as a result of the deaths caused by the virus. The proportion of the population that is vulnerable to the virus decreases exponentially, as seen in (Figures 3 & 4) shows that the vulnerable population steadily declines. The fact that nearly everyone in a group is infected indicates a stable endemic equilibrium condition. (Figure 5): As a result of a rise in resistance to COVID-19 With better prevention and treatment comes a larger vulnerable population. Because of a rise in resistance to COVID-19 (Figure 6). As immunity and treatment improve, it is shown that the quarantined population diminishes. Immunity to COVID-19 rises, as seen in (Figure 7). As the number of people who are immune to the disease and receiving treatment grows, the number of those who are exposed drops. (Figure 8): As a result of a rise in resistance to COVID-19, It has been shown that when immunity and treatment improve, the infectious population declines. Because of a rise in resistance to COVID-19, as seen in (Figure 9). It has been noted that as treatment and immunity improve, more people will recover. Because of a rise in resistance to COVID-19, as seen in (Figure 10).creases as the immunity and treatment increases.

DOI: 10.26717/BJSTR.2023.51.008046

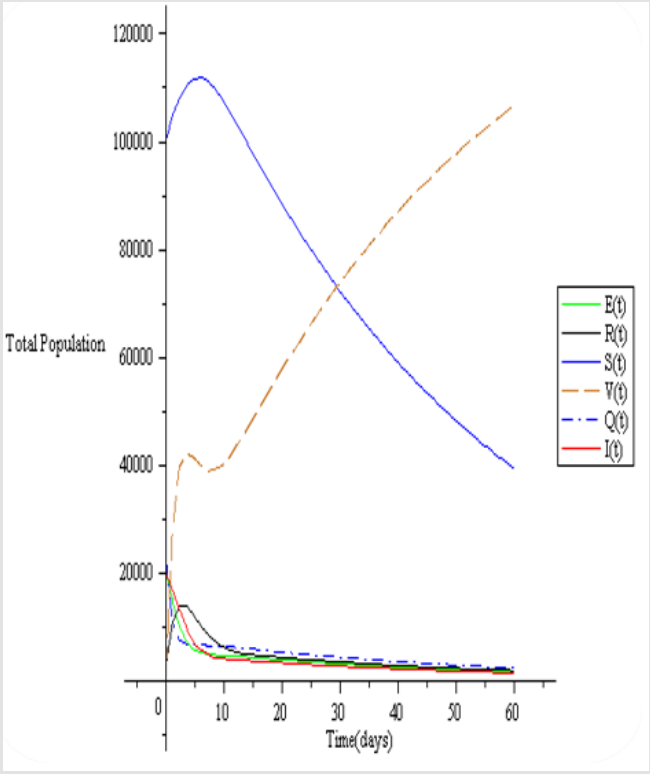

Figure 2: Transmission dynamics of COVID-19 infections between human population and the environment within the first 60 days.

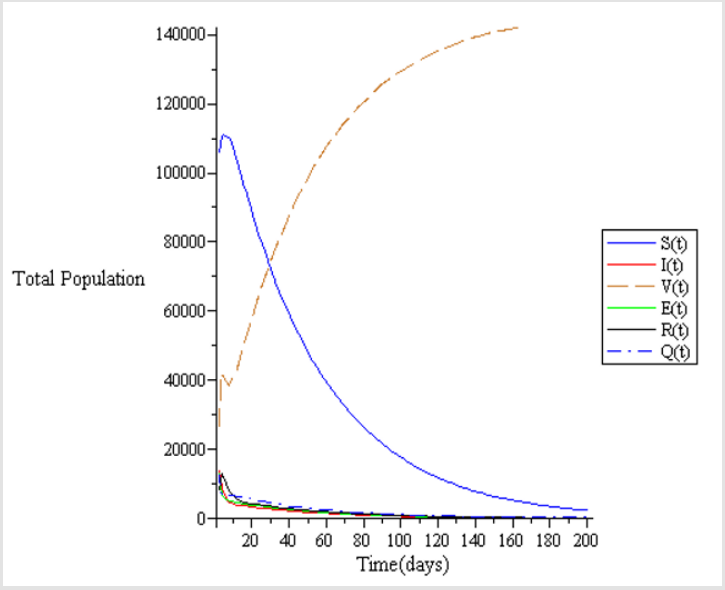

Figure 3: Transmission dynamics of COVID-19 infections between human population and the environment (within 200 days).

DOI: 10.26717/BJSTR.2023.51.008046

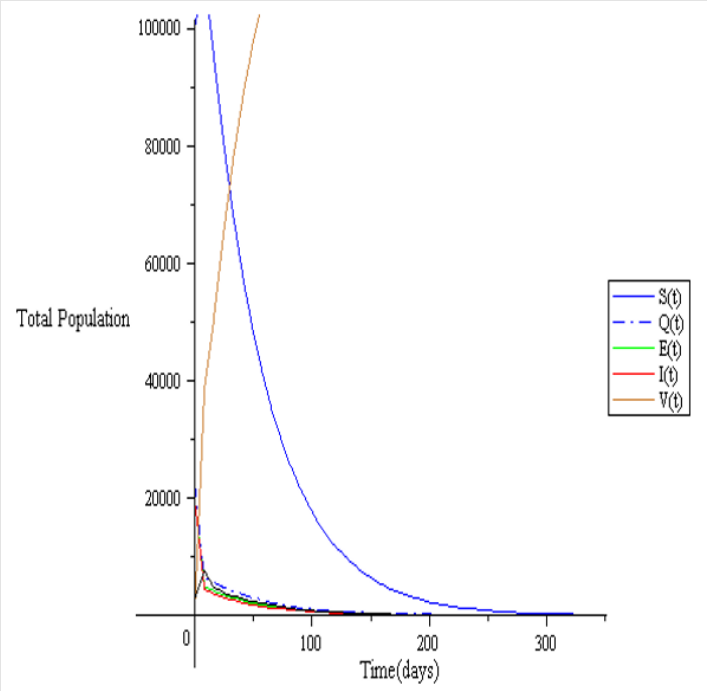

Figure 4: Transmission dynamics of COVID-19 infections between human population and the environment (after 200 days)

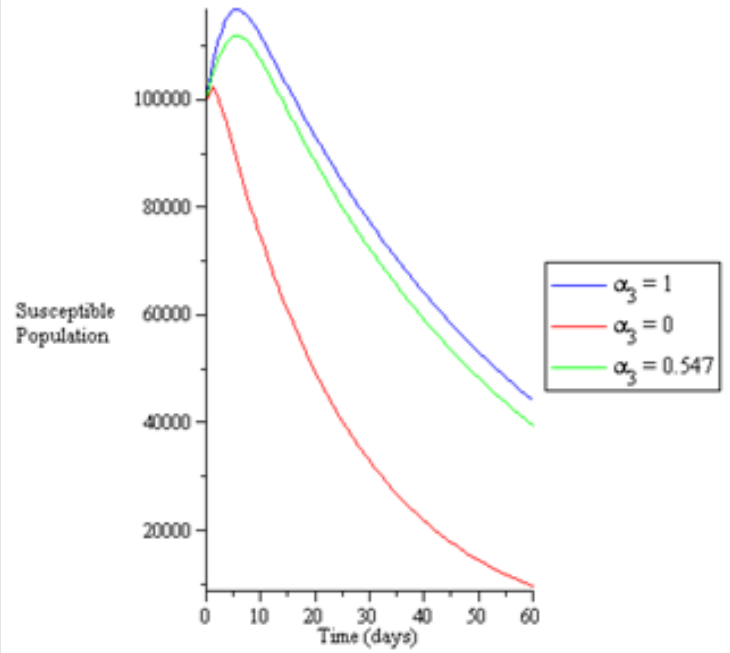

Figure 5: Effect of varying recovery rate α_3 (from natural immunity and treatment) on susceptible population

DOI: 10.26717/BJSTR.2023.51.008046

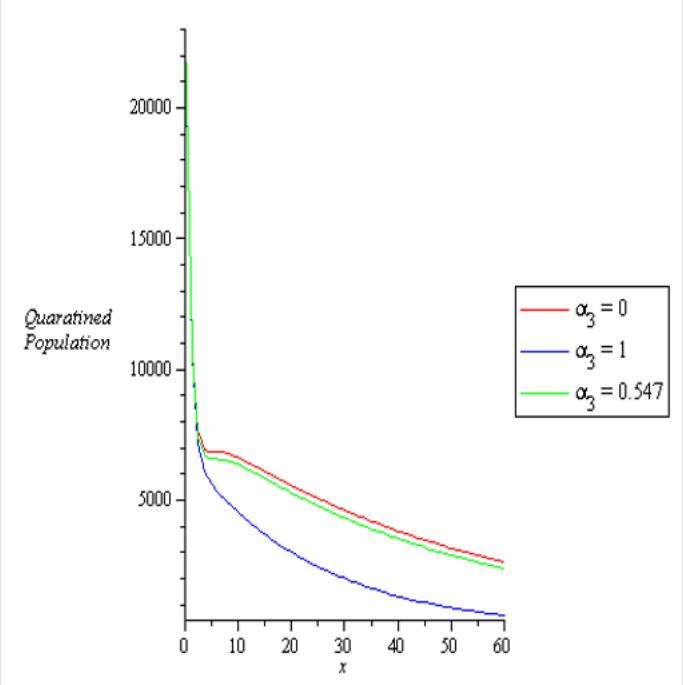

Figure 6: Effect of varying recovery rate α_3 (from natural immunity and treatment) on Quarantined population

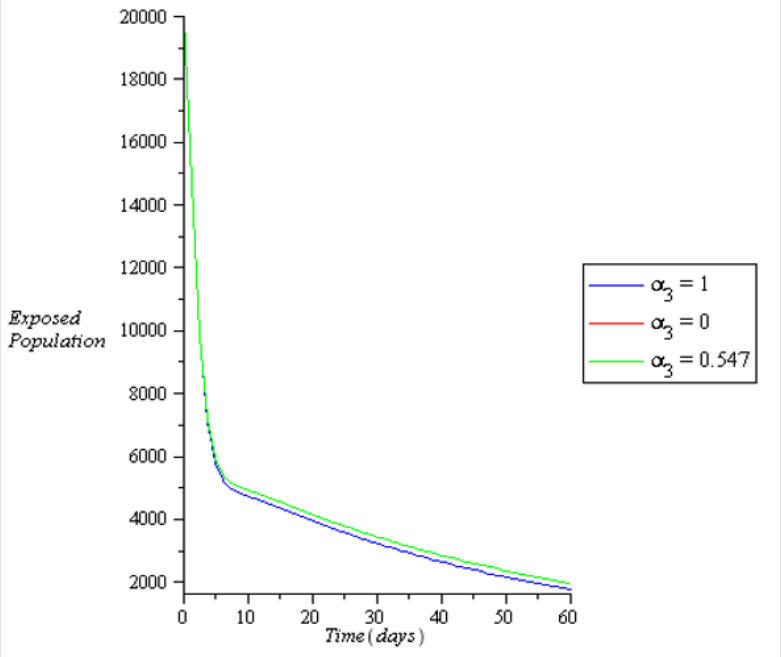

Figure 7: Effect of varying recovery rate α_3 (from natural immunity and treatment) on exposed population

DOI: 10.26717/BJSTR.2023.51.008046

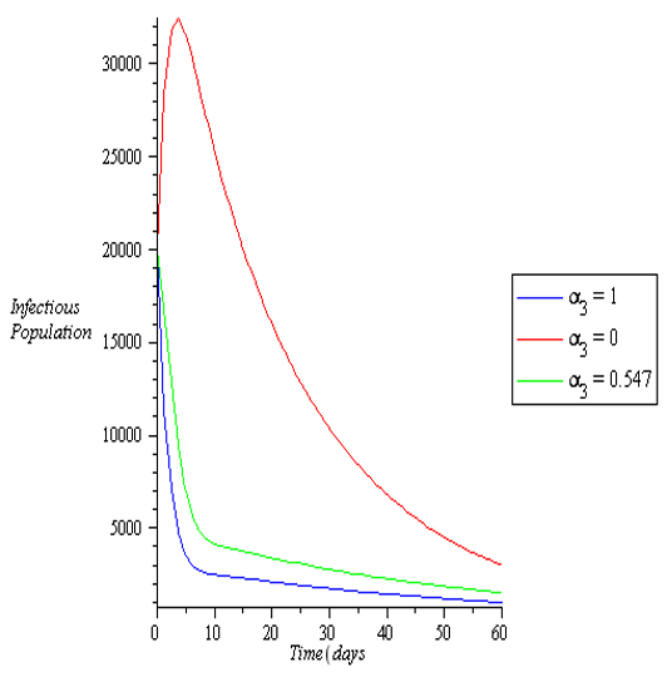

Figure 8: Effect of varying recovery rate α_3 (from natural immunity and treatment) on infectious population.

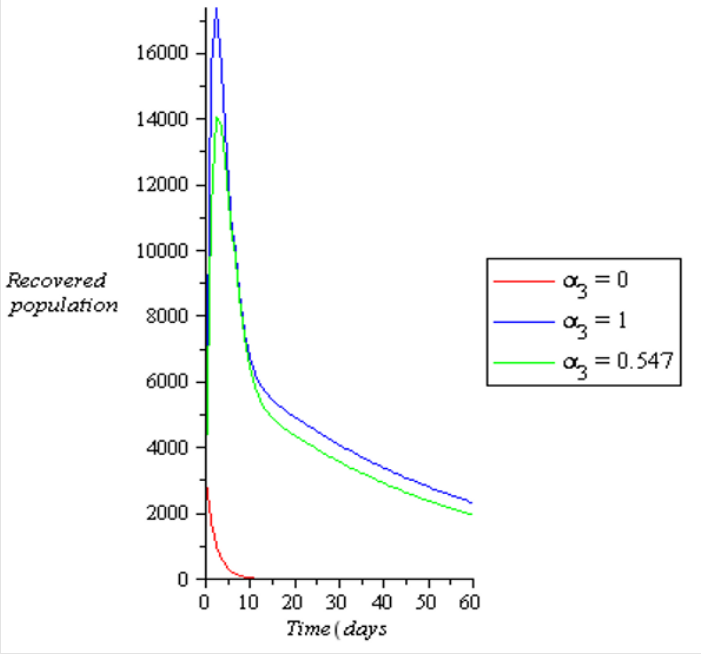

Figure 9: Effect of varying recovery rate α_3 (from natural immunity and treatment) on recovered population.

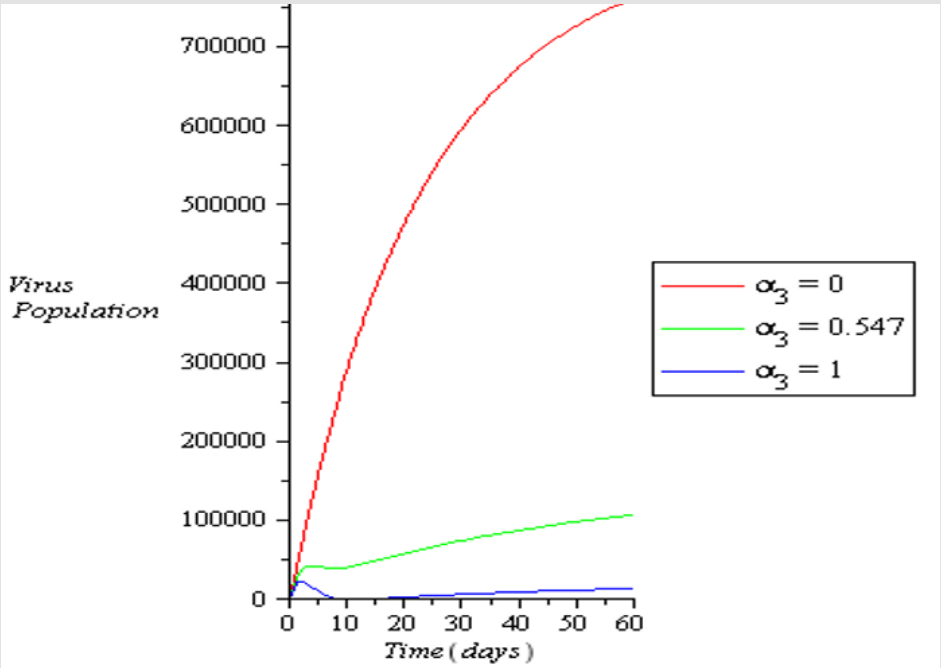

Figure 10: Effect of varying recovery rate α_3 (from natural immunity and treatment) on virus population in the environment.

Conclusion

This study focused on the transmission dynamics of COVID-19 [41]. We have proposed a non-linear mathematical model to consider the transmission dynamics and the impact of increase immunity and treatment on controlling the transmission dynamics of COVID-19 [42]. The positivity and boundedness, stability analysis and reproduction number where all analytically solved for. It is established that Disease free equilibrium point is stable if $R_0 < 1$ and that the endemic equilibrium state exist only if $R_0 > 1$.The study also revealed that increase in immunity and treatment cause significant decrease in quarantined population, exposed population, infectious population and virus in the environment, while it caused increase in susceptible population and recovered population [43].

Recommendation

Based on the findings of this study and on the imminent global second wave, we recommend governments and relevant agencies should provide adequate health facilities [44-47].to increase the rate of treatment and intensify public awareness on the positive effect of maintaining considerable physical distance, the use of face mask, avoid touching surface and constant application of hand sanitizers when in public places.

References

1. AC Loyinmi, KO Idowu (2023) Semi-Analytic Approach to Solving Rosenau-Hyman and Korteweg-De Vries Equations Using Integral Transform. Tanzania J. Sci 49(1): 26-40.
2. AC Loyinmi, LM Erinle Ibrahim, AE Adeyemi (2017) The new iterative method (NIM) for solving telegraphic equation. J. Niger. Assoc. Math. Phys 43: 31-36.
3. AC Loyinmi, OW Lawal, DO Sottin (2017) Reduced differential transform method for solving partial integro-differential equation. J. Niger. Assoc. Math. Phys 43: 37-42.
4. AC Loyinmi, OW Lawal (2011) The Asymptotic Solution for the Steady Variable-Viscosity Free Convection Flow on a Porous Plate. J. Niger. Assoc. Math. Phys 19.
5. AC Loyinmi, TK Akinfe (2020) An algorithm for solving the Burgers–Huxley equation using the Elzaki transform. SN Appl. Sci 2: 1-17.
6. AC Loyinmi, TK Akinfe (2020) Exact solutions to the family of Fisher's reaction-diffusion equation using Elzaki homotopy transformation perturbation method. Eng. Reports 2(2): e12084.
7. AO Babajide, IK Oluwatobi (2021) On The Elzaki Substitution And Homotopy Pertubation Methods For Solving Partial Differential Equation Involving Mixed Partial Derivatives. Fudma J. Sci 5: 159-168.
8. Anthony R F, Stanley P (2015) Coronaviruses: An overview of their replication and pathogenesis. Corona viruses 1282: 1-23.
9. Gallagher T M, Buchmeier MJ (2001) Coronavirus spike proteins in viral entry and pathogenesis. Virology 279(2): 371-374.
10. Hassan S, Sheikh F N, Jamal S, Ezeh J K, Akhtar A (2020) Coronavirus

(COVID-19): A Review of Clinical Features, Diagnosis, and Treatment. Cureus 12(3): e7355.

11. Atri D, Siddiqi H K, Lang J, Nauffal V, Morrow D A, et al. (2020) COVID-19 for the Cardiologist: A Current Review of the Virology, Clinical Epidemiology, Cardiac and Other Clinical Manifestations and Potential Therapeutic Strategies. JACC Basic Transl Sci 5(5): 518-536.
12. Rismanbaf A (2020) Potential Treatments for COVID-19; a Narrative Literature Review. Arch Acad Emerg Mede 8(1): e29.
13. Adeniyi M O, Ekum M I, Iluno C, Ogunsanya A S, Akinyemi J A, et al. (2020) Dynamic model of COVID-19 disease with exploratory data analysis. Scientific African, pp. 477.
14. Barlan A, Zhao J, Sarkar M K, Li K, McCray Jr P B, et al. (2014) Receptor variation and susceptibility to Middle East respiratory syndrome coronavirus infection. J Virol 88(9): 4953-4961.
15. Bermingham A, Chand M A, Brown C S, Aarons E, Tong C, et al. (2012) Severe respiratory illness caused by a novel coronavirus, in a patient transferred to the United Kingdom from the Middle East. Euro Surveill 17(40): 20290.
16. Brauer F (2017) Mathematical epidemiology: Past, present, and future. Infectious Disease Modelling 2(2): 113-127.
17. CE Overton, RR Wilkinson, A Loyinmi, JC Miller, KJ Sharkey, et al. (2022) Approximating quasi-stationary behaviour in network-based SIS dynamics. Bull. Math. Biol 84: 1-32.
18. Chen L, Liu M, Zhang Z, Qiao K, Huang T, et al. (2020) Ocular manifestations of a hospitalised patient with confirmed. Br J Ophthalmol 104(6): 748-751.
19. Chen T M, Rui J, Wang Q P, Zhao Z Y, Cui J A, et al. (2020) A mathematical model for simulating the phase-based transmissibility of a novel coronavirus. Infectious Diseases of Poverty 9(1): 24.
20. Cheng Y LR, Wang K, Zhang M, Wang Z, Dong L, et al. (2020) Kidney disease is associated with in-hospital death of patients with COVID-19. Kidney International 97(5): 829-838.
21. Chowell G, Abdirizak F, Lee S, Lee J, Jung E, et al. (2015) Transmission characteristics of MERS and SARS in the healthcare setting: a comparative study. BMC Med 13: 210.
22. DO Odulaja, LM Erinle Ibrahim, AC Loyinmi (2013) Numerical computation and series solution for mathematical model of HIV/AIDS Computation and series solution for mathematical model of HIV/AIDS. Scienpress Ltd.
23. de Groot R, Baker S, Baric R, Enjuanes L, Gorbalenya A, et al. (2012) Family Coronaviridae. In: King A, Adams M, Cartens E, Lefkowitz E (Eds.)., Virus Taxonomy; Ninth Report of the International Committee on Taxonomy of Viruses. San Diego: Academic, pp. 806-28.
24. de Wilde AH, Snijder EJ, Kikkert M, van Hemert MJ (2018) Host factors in coronavirus replication. Curr Top Microbiol Immunol 419: 1-42.
25. Drexler J F, Corman V M, Drosten C (2014) Ecology, evolution and classification of bat coronaviruses in the aftermath of SARS. Antiviral Res 101: 45-56.
26. EIL Morenikeji, AO Babajide, IK Oluwatobi (2021) Application Of Homotopy Perturbation Method To The Mathematical Modelling Of Temperature Rise During Microwave Hyperthermia. Fudma J. Sci. 5(2): 273-282.
27. Fang Y, Nie Y, Penny P (2020) Transmission dynamics of the covid-19 outbreak and effectiveness of government interventions: A data-driven analysis. Journal of Medical Virology 92(6): 645-659.
28. Giovanetti M, Benvenuto D, Angeletti S, Ciccozzi M (2020) he first two cases of 2019- nCoV in Italy: where they come from? J Med Virol 92(5): 518-521.
29. Guan W J, Ni Z Y, Hu Y, Liang W H, Ou C Q, et al. (2020) Clinical Characteristics of Coronavirus Disease 2019 in China. The New England journal of medicine 382: 1708-1720.
30. H Wang, Z Wang, Y Dong, R Chang, C Xu, et al. (2020) Phase-adjusted estimation of the number of coronavirus disease 2019 cases in wuhan, china. Cell Discovery 6(1): 1-8.
31. H Yasmin, N Iqbal (2022) A Comparative Study of the Fractional-Order Nonlinear System of Physical Models via Analytical Methods. Math. Probl. Eng 2022.
32. Hamming I, Timens W, Bulthuis ML, Lely AT, Navis G, et al. (2004) Tissue distribution of ACE2 protein, the functional receptor for SARS coronavirus. A first step in understanding SARS pathogenesis. J Pathol 203(2): 631-637.
33. Hampton T (2005) Bats may be SARS reservoir. JAMA 294(18): 2291.
34. Huang X, Dong W, Milewska A, Golda A, Qi Y, et al. (2015) Human Coronavirus HKU1 Spike Protein Uses OAcetylated Sialic Acid as an Attachment Receptor Determinant and Employs Hemagglutinin-Esterase Protein as a Receptor-Destroying Enzyme. J Virol 89(14): 7202-7213.
35. Hussain S, Pan J, Chen Y, Yang Y, Xu J, et al. (2005) Identification of novel subgenomic RNAs and noncanonical transcription initiation signals of severe acute respiratory syndrome coronavirus. J Virol 79(9): 5288-5295.
36. JO Agbomola, AC Loyinmi (2022) Modelling the impact of some control strategies on the transmission dynamics of Ebola virus in human-bat population: An optimal control analysis. Heliyon 8(12): e12121.
37. Jia HP, Look DC, Shi L, Hickey M, Pewe L, et al. (2005) ACE2 receptor expression and severe acute respiratory syndrome coronavirus infection depend on differentiation of human airway epithelia. J Virol 79(23): 14614-14621.
38. Jin Y H, Cai L, Cheng Z S, Cheng H, Deng T, et al. (2020) A rapid advice guideline for the diagnosis and treatment of 2019 novel coronavirus (2019- nCoV) infected pneumonia (standard version). Mil Med Res 7(1): 4.
39. KO Idowu, TG Akinwande, I Fayemi, UM Adam, AC Loyinmi, et al. (2023) Laplace Homotopy Perturbation Method (LHPM) for Solving Systems of N-Dimensional Non-Linear Partial Differential Equation. 3(1).
40. KT Akinfe, AC Loyinmi (2020) Stability analysis and semi-analytic solution to a SEIR-SEI Malaria transmission model using He's variational iteration method.
41. KT Akinfe, AC Loyinmi (2021) The Implementation of an Improved Differential Transform Scheme on the Schrodinger Equation Governing Wave-Particle Duality in Quantum Physics and Optics. Available SSRN 4098920 40.
42. Kang C K, Song K H, Choe P G, Park W B, Bang J H, et al. (2017) Clinical and epidemiologic characteristics of spreaders of middle east respiratory syndrome coronavirus during the 2015 outbreak in Korea. J Korean Med Sci 32(5): 744-749.
43. LM Erinle Ibrahim, AI Adewole, C Loyinmi, OK Sodeinde (2020) AN OPTIMIZATION SCHEME USING LINEAR PROGRAMMING IN A PRODUCTION LINE OF RITE FOODS LIMITED OSOSA. FUDMA J. Sci 4(1): 502-510.
44. Lawal OW, Loyinmi AC (2019) Laplace Homotopy Perturbation Method For Solving Coupled System Of Linear And Nonlinear Partial Differential Equation.

45. Lee P I, Hsueh P R (2020) Emerging threats from zoonotic coronaviruses-from SARS and MERS to 2019-nCoV. J Microbiol Immunol Infect 53(3): 365-367.

46. Letko M, Marzi A, Munster V (2020) Functional assessment of cell entry and receptor usage for SARS-CoV-2 and other lineage B betacoronaviruses. Nat Microbiol 5(4): 562-569.

47. Li W, Shi Z, Yu M, Ren W, Smith C, Epstein J H (2005) Bats are naturalreservoirs of SARS-like coronaviruses. Science 310(5748): 676-679.

48. Li W, Moore M J, Vasilieva N, Sui J, Wong S K, et al. (2003) Angiotensin-converting enzyme 2 is a functional receptor for the SARS coronavirus. Nature 426(6965): 450-454.

49. Liu Y, Chen H, Tang K, Guo Y (2020) Clinical manifestations and outcome of SARS CoV-2 infection during pregnancy. J Infect S0163-4453(20): 30109-30102.

50. Lu H, Stratton C, Tang Y (2020) Outbreak of pneumonia of unknown etiology in Wuhan, China: the mystery and the miracle. J Med Virol 92(4): 401-402.

51. M Alesemi, N Iqbal, AA Hamoud (2022) The Analysis of Fractional-Order Proportional Delay Physical Models via a Novel Transform. Complexity 2022.

52. M Erinle Ibrahim Latifat, IK Oluwatobi, I Sulola Abigail (2021) Mathematical modelling of the transmission dynamics of malaria infection with optimal control. Kathmandu Univ. J. Sci. Eng. Technol 15.

53. M Suleman, T Elzaki, Q Wu, N Anjum, JU Rahman, et al. (2017) New application of Elzaki projected differential transform method, J. Comput. Theor. Nanosci. 14(1): 631-639.

54. Millet J K, Whittaker G R (2015) Host cell proteases: critical determinants of coronavirus tropism and pathogenesis. Virus Res 202: 120-34.

55. Mizumoto K, Chowell G (2020) Estimating risk for death from 2019 novel coronavirus disease, china, january-february 2020. Emerging Infectious Diseases 26(6): 1251-1256.

56. OO Lawal, AC Loyinmi, OS Sowunmi (2017) Homotopy perturbation algorithm using laplace transform for linear and nonlinear ordinary delay differential equation. J. Niger. Assoc. Math. Phys 41: 27-34.

57. OW Lawal, AC Loyimi (2019) Application of new iterative method for solving linear and nonlinear initial boundary value problems with non local conditions. Sci. World J 14(3): 100-104.

58. OW Lawal, AC Loyimi, Erinle Ibrahim (2018) Algorithm for Solving a Generalized Hirota-Satsuma Coupled KDV Equation Using Homotopy Perturbation Transform Method. Sci. World J 13(3).

59. OW Lawal, AC Loyinmi, AR Hassan (2019) Finite difference solution for magnetohydrodynamics thin film flow of a third-grade fluid down inclined plane with ohmic heating. ABACUS 46: 92-97.

60. OW Lawal, AC Loyinmi, DA Aruba (2017) Approximate solutions of higher dimensional linear and nonlinear initial boundary valued problems using new iterative method. J Niger. Assoc Math Phys 41: 35-40.

61. Olaniyi S, Okosun K O, Adesanya S O, Areo E A (2018) Global stability and optimal control analysis of malaria dynamics in the presence of human travelers. The Open Infectious Diseases Journal 10(1): 166-186.

62. Peiris J S, Lai S T, Poon L L, Guan Y, Yam L Y, et al. (2003) Coronavirus as a possible cause of severe acute respiratory syndrome. Lancet 361(9366): 1319-1325.

63. Perrier A, Bonnin A, Desmarets L, Danneels A, Goffard A, et al. (2019) The C terminal domain of the MERS coronavirus M protein contains a trans-Golgi network localization signal. J Biol Chem 294(39): 14406-14421.

64. Raj V S, Mou H, Smits S L, Dekkers D H, Muller M A, et al. (2013) Dipeptidyl peptidase 4 is a functional receptor for the emerging human coronavirus-EMC. Nature 495(7440): 251-254.

65. Sawicki S G, Sawicki D L (2005) Coronavirus transcription: a perspective. Curr Top Microbiol Immunol 287: 31-55.

66. Simmons G, Gosalia D N, Rennekamp A J, Reeves J D, Diamond S L, et al. (2005) Inhibitors of cathepsin L prevent severe acute respiratory syndrome coronavirus entry. P Natl Acad Sci USA 102(33): 11876-11881.

67. Song H D, Tu C C, Zhang G W, Wang S Y, Zheng K, et al. (2005) Cross-host evolution of severe acute respiratory syndrome coronavirus in palm civet and human. Proc Natl Acad Sci USA 102(7): 2430-2435.

68. Song W, Gui M, Wang X, Xiang Y (2018) Cryo-EM structure of the SARS coronavirus spike glycoprotein in complex with its host cell receptor ACE2. PLoS Pathog 14(8): e1007236.

69. TK Akinfe, AC Loyinmi (2021) A solitary wave solution to the generalized Burgers-Fisher's equation using an improved differential transform method: A hybrid scheme approach, Heliyon 7(5): e07001.

70. TK Akinfe, AC Loyinmi (2022) An improved differential transform scheme implementation on the generalized Allen–Cahn equation governing oil pollution dynamics in oceanography. Partial Differ. Equations Appl. Math 6: 100416.

71. Wong H H, Kumar P, Tay F P L, Moreau D, Liu D X, et al. (2015) Genome-Wide Screen Reveals Valosin-Containing Protein Requirement for Coronavirus Exit from Endosomes. J Virol 89(21): 11116-11128.

72. Woo P C, Lau S K, Lam C S, Lau C C, Tsang A K, et al. (2012) Discovery of seven novel Mammalian and avian coronaviruses in the genus delta coronavirus supports bat coronaviruses as the gene source of alpha coronavirus and beta coronavirus and avian coronaviruses as the gene source of gamma coronavirus and delta coronavirus. J Virol 86(7): 3995-4008.

73. Woo P C, Lau S K, Lam C S, Lau C C, Tsang A K, et al. (2012) Discovery of seven novel Mammalian and avian coronaviruses in the genus delta coronavirus supports bat coronaviruses as the gene source of alpha coronavirus and beta coronavirus and avian coronaviruses as the gene source of gamma coronavirus and delta coronavirus. J Virol 6(7): 3995-4008.

74. Wu F, Zhao S, Yu B, Chen Y M, Wang W, et al. (2020) A new coronavirus associated with human respiratory disease in China 579(7798): 265-269.

ISSN: 2574-1241

DOI: 10.26717/BJSTR.2023.51.008046

Idowu Kabir Oluwatobi. Biomed J Sci & Tech Res

Submission Link: https://biomedres.us/submit-manuscript.php